


Effect of X-ray irradiation on the optical properties of nanostructured thin films TCVA based on structural analysis

A. A. A. Darwish^{1,2} · Shams A. M. Issa^{1,3} · Taymour A. Hamdalla^{1,4}  · M. M. El-Nahass⁵

Received: 28 May 2017 / Accepted: 7 November 2017 / Published online: 10 November 2017
© Springer Science+Business Media, LLC, part of Springer Nature 2017

Abstract Nanocrystalline thin films of 4-tricyanovinyl-*N,N*-diethylaniline (TCVA) were prepared by the thermal evaporation method. TCVA thin films were irradiated by X-ray radiation at room temperature with different absorbed doses up to 2500 Gy. The structural properties of TCVA pre and post irradiation have been investigated using Fourier-transform infrared and X-ray diffraction. Spectrophotometric measurements were utilized to study the optical transmittance and optical reflectance for TCVA, pre and post irradiation and consequently optical parameters were calculated. At 850 nm, the refractive index of TCVA thin films increases by approximately 16% when the dose increases from 0 to 2500 Gy. It is found that a slight modification in the energy band gap occurred while a significant change appeared in the refractive index. These results are useful for the manufacture of diffractive optical components or integrated optical parts.

Keywords Organic compounds · Optical constants · X-ray irradiation

✉ Taymour A. Hamdalla
taymour_76@yahoo.com

¹ Nanotechnology Research Laboratory, Department of Physics, Faculty of Science, University of Tabuk, Tabuk, Saudi Arabia

² Department of Physics, Faculty of Education at Al-Mahweet, Sana'a University, Al-Mahweet, Yemen

³ Department of Physics, Faculty of Science, Al-Azhar University, Assiut, Egypt

⁴ Department of Physics, Faculty of Science, Alexandria University, Alexandria, Egypt

⁵ Department of Physics, Faculty of Education, Ain Shams University, Rorxy, Cairo 11757, Egypt

1 Introduction

Commercially, the organic materials play a vital role in the field of plastic electronics. The organic materials gain its significant properties because of the small-molecule organic semiconductors as in organic photovoltaic cells, organic light emitting diodes and organic field-effect transistors (Anthony et al. 2010; Goetz et al. 2011; Lehnherr et al. 2012; Mei et al. 2013). Tricyanovinyl derivatives are considered one of the most promising conductive organic materials which have a high ability transfer charges in the electronic ground state. In the optical sensing field, tricyanovinyl groups are very sensitive to nucleophilic attacks (El-Nahass et al. 2009a). 4-tricyanovinyl-*N,N*-diethylaniline (TCVA) is a donor–acceptor disubstituted benzenes dye, which classifies as an organic molecular rotors compound. TCVA gives rise to high potential applications in the optoelectronic devices and in nonlinear optics such as data storage (El-Nahass et al. 2009b, c). Furthermore, it has a great importance in coloring synthetic polymer fibers. TCVA was used as a sublime dye in photoconductive recording materials and in heat-transfer recording materials (El-Nahass et al. 2009a; Deshpande et al. 1990). Organic materials easily be processed using a spin coating or evaporation techniques. The evaporating technique can be used to produce thin films from pure metals, alloys, and organic compounds (El-Nahass et al. 2009a).

Sensitivity of the organic materials towards radiation has been discussed much during the last two decades (El-Mallawany et al. 1998; Hamdalla and Nafee 2014; Arshak and Korostynska 2004; El-Nahass et al. 2013). X-rays are considered part of the ionizing radiation which causes different effects on the organic materials. In fact, the molecular structure of most of the organic materials have been found to degrade when exposed to ultraviolet and X-ray radiation (Nafee et al. 2017; Egerton et al. 2014). X-rays cause changes in the structure of the organic material known as nuclear transmutation, radiolysis, and ionization (Jouhara et al. 2009). X-ray irradiation leads to a clear changes in the optical and electrical properties of the organic materials.

The present experimental work aims at describing the effects of X-ray irradiation on the structural and optical properties of TCVA nanostructure films, including the influence on the optical parameters. Finally, we calculate the optical constants of TCVA nanostructure thin films.

2 Experimental details

TCVA compound has been synthesized by reacting tetracyanoethylene and *N,N*-diethylaniline, as previously explained by El-Nahass et al. (2009c). Thin films of TCVA were fabricated by using thermal evaporation methods utilizing a coating unit (Edwards E306A), onto optically and ultrasonically cleaned flat glass, quartz and cleaved KBr single crystal substrates. For IR measurements, we deposited TCVA on KBr substrates, while the glass substrates were used for depositing films for the X-ray diffraction (XRD). The optically flat amorphous quartz substrates were used for the optical measurements. The substrate was settled onto a rotatable holder to get homogeneous fabricated films at a separation of 25 cm over the evaporator. The TCVA thin film was fabricated using Edward E306A coating unit under vacuum greater than 10^{-4} Pa. The substrate was kept at room temperature. The quartz crystal thickness was 315 nm and the deposition rate was 5 nm/s. The film thickness was checked by using the interferometric method. To

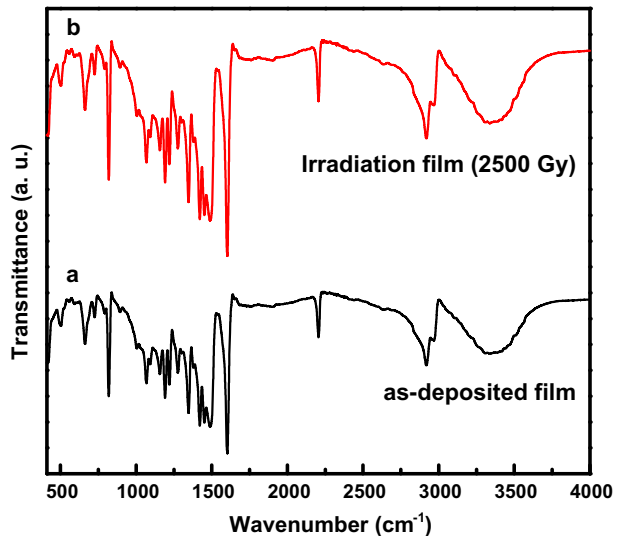
study the effect of radiation on thin films, the as-deposited samples were exposed, in air, to high-energy X-ray (6 MeV). The irradiation dose (up to 2500 kGy) was applied using Philips X-ray diffractometer (model X' Pert) linear accelerator (Philips electronics UK version SL15).

The Fourier-transform infrared (FTIR) in the spectral range 400–4000 cm^{-1} was used to check the chemical structures of TCVA thin films for doses up to 2500 Gy. During the experimental method, the infrared spectrophotometer spectral resolution is $\pm 1 \text{ cm}^{-1}$. XRD was applied to test the characteristics of TCVA structure. X-ray diffraction patterns (XRD) were used to investigate the characteristics of TCVA structure. The patterns of XRD analysis were run using Philips Diffractometer 1710 in the normal 2θ (degree) scan with $\text{CuK}\alpha$ radiation ($\lambda = 1.54178 \text{ \AA}$) at 40 kV and 30 mA with a scanning speed of 2 degrees/min.

Beforehand, the crystal structure of TCVA powder has been explored by XRD and it is found to possess triclinic structure. The evaporation of TCVA prompted a film which had a specific level of crystallinity (El-Nahass et al. 2013). The surface morphology of our TCVA samples have been previously examined using SEM micrograph and it has been confirmed by our team that the size of crystallites (grain size) could be referred as a part of “morphology” as reported in (El-Nahass et al. 2013).

The optical transmittance (T) and reflectance (R) spectra of the prepared thin films were measured by double beam spectrophotometer model V-670 JASCO in the wavelength range 200–2500 nm, with a resolution is $\pm 0.1 \text{ nm}$. On the basis of T and R , the optical constants such as refractive index, n , and absorption index, k , have been calculated by using Murmann's exact equations (El-Nahass et al. 2009a). The experimental errors were found to be $\pm 2\%$ for film thickness, $\pm 1\%$ for T & R , $\pm 2.3\%$ for n and 2.1% for k (El-Nahass et al. 1997).

Fig. 1 Infrared spectra of TCVA for the **a** as-deposited film, **b** irradiated film at 2500 Gy



3 Results and discussion

FT-IR is an analytical technique used to identify organic, polymeric, and in some cases, inorganic materials. FTIR spectra exhibit several absorption bands of stretching and bending vibrations for C–C, C–H, C=C and C≡N groups within TCVA. Figure 1 illustrates the absorption spectra of pre and post X-ray irradiated TCVA thin films in the range 400–4000 cm^{-1} . This figure shows a broad band at 3368.2 cm^{-1} due to a hydroxyl group O–H stretching vibration for deposited and irradiated TCVA thin films. C–H aromatic band absorption appeared at 3000 cm^{-1} . Two absorption bands at 2973.7 and 2919.7 cm^{-1} are assigned to an asymmetric C–H stretching mode of the CH₃ group and C–H asymmetric stretching in CH₂, respectively. At 2202.3 cm^{-1} , a sharp absorption band that appeared was assigned to the stretching vibration of C≡N group that forms conjugated bond with the benzene ring. Due to the C=C stretching vibration a strong band appears at 1600.6 cm^{-1} . The peaks at 1450 cm^{-1} and 1367.8 cm^{-1} indicate to the CH₃ bending modes. The C–H deformation bands of aromatic C–H groups are observed at 819.6 and 792.7 cm^{-1} . The bands in the 792.7–679 cm^{-1} region can be assigned to C–H and C–C vibrations. Figure 1 shows that the as-deposited thin film spectra are similar to irradiated thin film spectra at the maximum dose which indicates the TCVA radiation resistance.

Figure 2 shows XRD of as-deposited and irradiated thin films. At $2\theta = 7.25^\circ$, the as-deposited thin film has only one peak (001) with the hump of amorphity in 17° – 35° . Figure 2 also indicates that the irradiation of our mentioned samples motivated nanocrystalline to amorphous phase transformation. This could be related to the disorder within our synthesized samples due to irradiation exposure.

Figure 3 illustrates *T* and *R* spectra of TCVA thin films pre and post irradiation with the wavelength range between 200 and 2500 nm. This figure shows two different behaviors, the first one at a longer wavelength ($\lambda > 1000$ nm) where the as-deposited and irradiated thin films are transparent and no light is scattered or absorbed ($R + T = 1$). The second region appears at a shorter wavelength ($\lambda < 1000$ nm) due to absorption. The effect of X-ray irradiation dose appears at approximately $\lambda > 850$ nm, where the intensity of transmittance decreases when X-ray irradiation dose increase. This is attributed to the

Fig. 2 X-ray diffraction of as-deposited and irradiated TCVA films

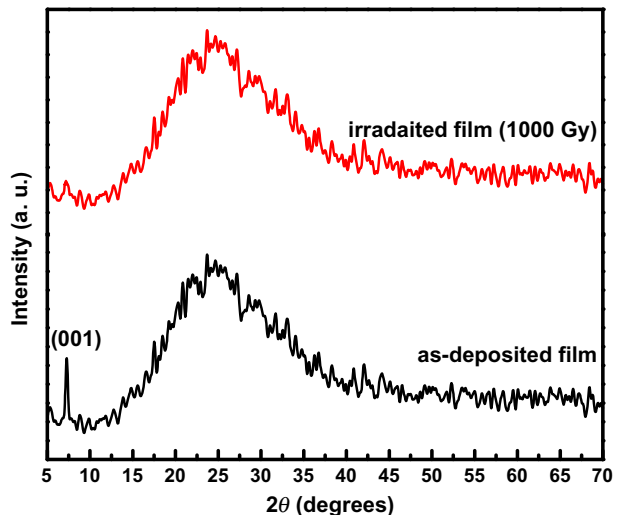
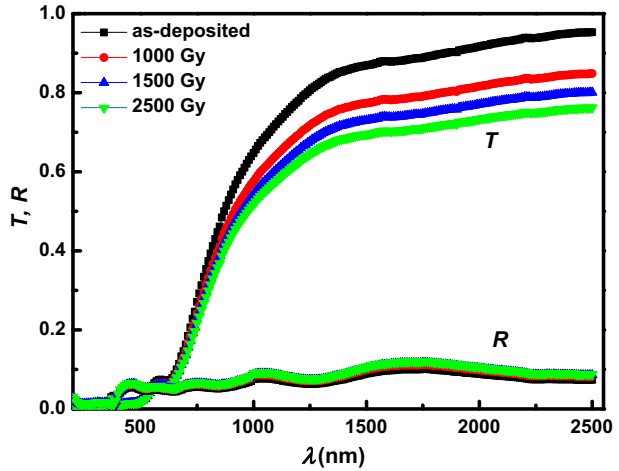


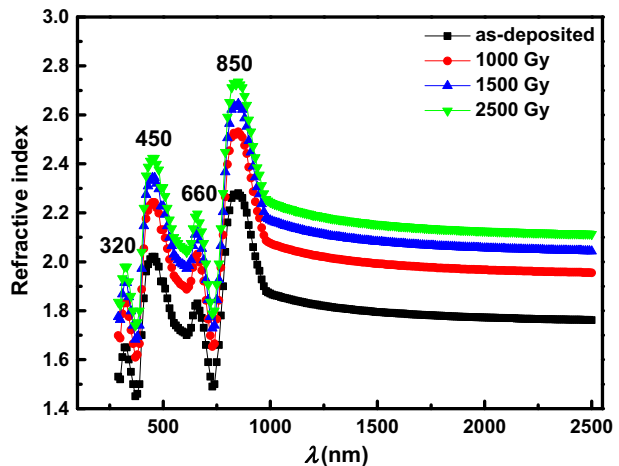
Fig. 3 The spectral distribution of normal incidence transmittance, T , and reflectance, R , for TCVA films with different X-ray doses



disorder increase within the synthesized samples. It was previously reported that, irradiation effect on organic thin film decreases the ordering character in the crystalline phases of organic main chain (Nafee et al. 2017).

Figure 4 shows the relation between the refractive index of TCVA thin films and the wavelength for X-ray doses up to 2500 Gy. The refractive index is dispersive for wavelengths less than 850 nm. This may be related to anomalous dispersion by the receiving multioscillator model. On the contrary, for wavelengths more than 850 nm, the refractive index changes slowly, which could be related to normal dispersion by the single oscillator model (El-Nahass et al. 2009a). As the X-ray radiation dose reached 2500 Gy, TCVA refractive index increased from 1.65, 2.02, 1.83, and 2.28 to 1.98, 2.42, 2.20 and 2.72 at λ of 320, 450, 660 and 850 nm, respectively. The increase in the refractive index is associated with the exposure to X-rays radiation. This could be attributed to the radiation defects that appear in our synthesized sample. Also, the X-ray irradiation ionizes some of the organic molecules creating free radicals which interact with each other to form a cross linked structure (Haraguchi et al. 2015).

Fig. 4 Spectral behavior of refractive index (n) of the as-deposited and irradiated TCVA thin films



The refractive index dispersion of TCVA thin films is expressed as (El-Nahass et al. 2004; El-Nahass and Hassanien 2004)

$$n^2 = 1 + \frac{E_o E_d}{E_o^2 - (hv)^2}, \tag{1}$$

where E_o is the oscillator transitions energy, hv is the photon energy and E_d is the dispersion energy. By using this model, we can describe the dielectric response for transitions below the optical gap. The slope of the straight line for the relation between $1/(n^2 - 1)$ versus $(hv)^2$ in Fig. 5 represents E_o , while E_d is the interception with y-axis, whose values are given in Table 1. Moreover, the lattice dielectric constant (ϵ_L), describes the lattice vibration contribution model and the dispersion of free carriers. The dependence of dielectric constant (ϵ_I) on λ in the normal dispersion is represented by (El-Nahass et al. 2004; El-Nahass and Hassanien 2004)

$$\epsilon_I = n^2 = \epsilon_L - \frac{e^2}{4\pi^2 \epsilon_o c^2} \frac{N}{m^*} \lambda^2, \tag{2}$$

where e , ϵ_o and N/m^* are the elementary charge, the permittivity of free space and the ratio of free carrier concentration to the free carrier effective mass, respectively.

Figure 6 shows the relation between n^2 and λ^2 for TCVA thin films pre and post irradiation. It can be noted from the figure that there is a linear dependence of n^2 on λ^2 at a longer wavelength. The lattice dielectric constants for our samples were obtained by extrapolating the linear parts to zero wavelength, and the ratio N/m^* is equal to the slope of linear parts. As listed in Table 1, the high frequency dielectric constant (ϵ_∞), the lattice dielectric constant (ϵ_L), the single oscillator energy (E_o), the dispersion energy (E_d), and the N/m^* ratio all increase with increasing X-ray dose. This may be due to the effect of high irradiation on the bond length within our TCVA samples.

The absorption coefficient, α , can be calculated using the relation

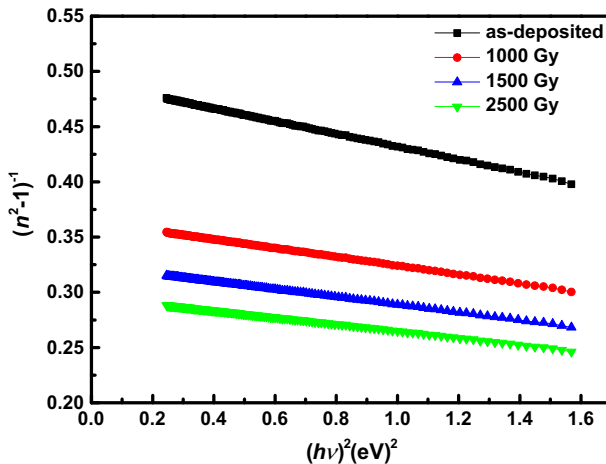


Fig. 5 Variation of $(n^2 - 1)^{-1}$ with $(hv)^2$ (eV)² of TCVA films different doses of irradiation

Table 1 Dispersion parameters of TCVA films

	ϵ_{∞}	ϵ_L	E_o (eV)	E_d (eV)	N/m^* ($10^{44} \text{ g}^{-1} \text{ cm}^{-3}$)
as-deposited	3.02 ± 0.03	3.27 ± 0.03	2.91 ± 0.03	5.96 ± 0.03	2.71 ± 0.03
1000 Gy	3.75 ± 0.03	3.98 ± 0.02	3.02 ± 0.03	8.31 ± 0.03	3.01 ± 0.03
1500 Gy	4.09 ± 0.02	4.37 ± 0.02	3.06 ± 0.02	9.47 ± 0.02	3.14 ± 0.03
2500 Gy	4.38 ± 0.02	4.66 ± 0.02	3.08 ± 0.02	10.42 ± 0.02	3.33 ± 0.03

Fig. 6 The relation between n^2 and λ^2 of as-deposited and irradiated TCVA thin films

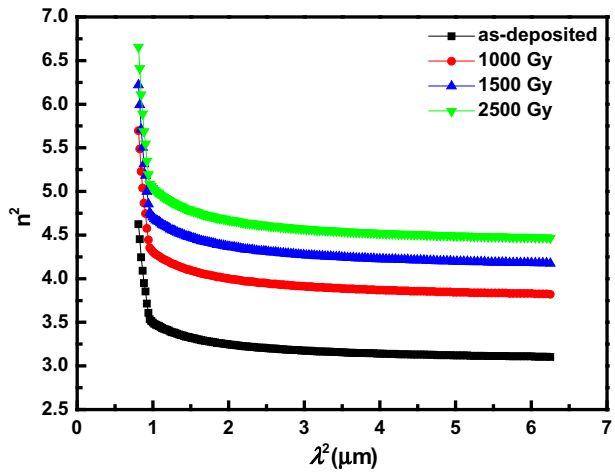
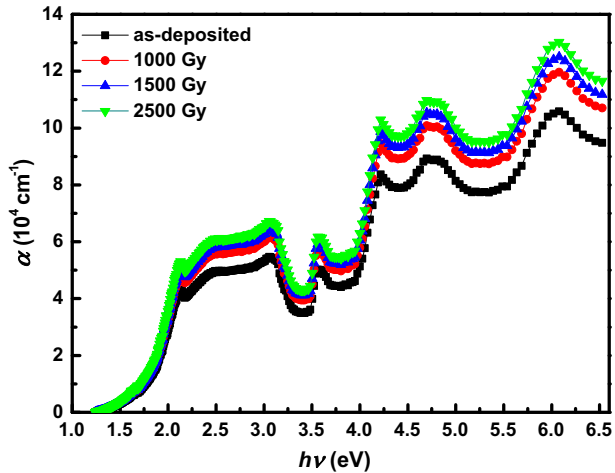


Fig. 7 Spectral behavior of absorption coefficient (α) as a function of photon energy ($h\nu$) for as-deposited and irradiated TCVA films



$$\alpha = \frac{4\pi k}{\lambda} \tag{3}$$

Figure 7 presents the relation of absorption coefficient with photon energy ($h\nu$) for as-deposited and irradiated TCVA thin films. It shows that the absorption coefficient has the

values in order of 10^4 cm^{-1} . It is clear that, the absorption coefficient increases with a X-ray dose ranging from 1000 to 2500 Gy.

The electron transition and E_g values were determined by using Bardeen's formula (El-Nahass et al. 2004; El-Nahass et al. 1988)

$$(\alpha h\nu)^r = B(h\nu - E_g) \quad (4)$$

where B is constant representing the electronic conductivity with level split and r is the transition process (r is a constant depends on the nature of the band to band electronic transitions and the electron density profile). Equation 4 has been used to fit to the experimental data at different values of r . The better fit was found to be at $r = 1/2$ (indirect allowed transitions). This behavior was modified by the following equation (El-Nahass et al. 2004):

$$(\alpha h\nu)^{\frac{1}{2}} = B(h\nu - E_g \pm E_{ph}) \quad (5)$$

where E_{ph} is the phonons assisted energy. Dependence of $(\alpha h\nu)^{\frac{1}{2}}$ on the photon energy ($h\nu$) for as deposited and irradiated TCVA films are shown in Fig. 8. The calculated values of E_g and E_{ph} are listed in Table 2. The optical energy gap values are 1.45, 1.41, 1.38, 1.35 eV corresponding to X-ray dose 0, 1000, 1500 and 2500 Gy, respectively. It means that, the optical energy gap depends on the X-ray radiation dose. The optical gap variation may arise from the disorder growing within our prepared material, and also due to deformities arising in the crystal field (El-Sayed 2004). The irradiation of TCVA thin film acts to decrease E_g which is related to the increases of the interatomic distance.

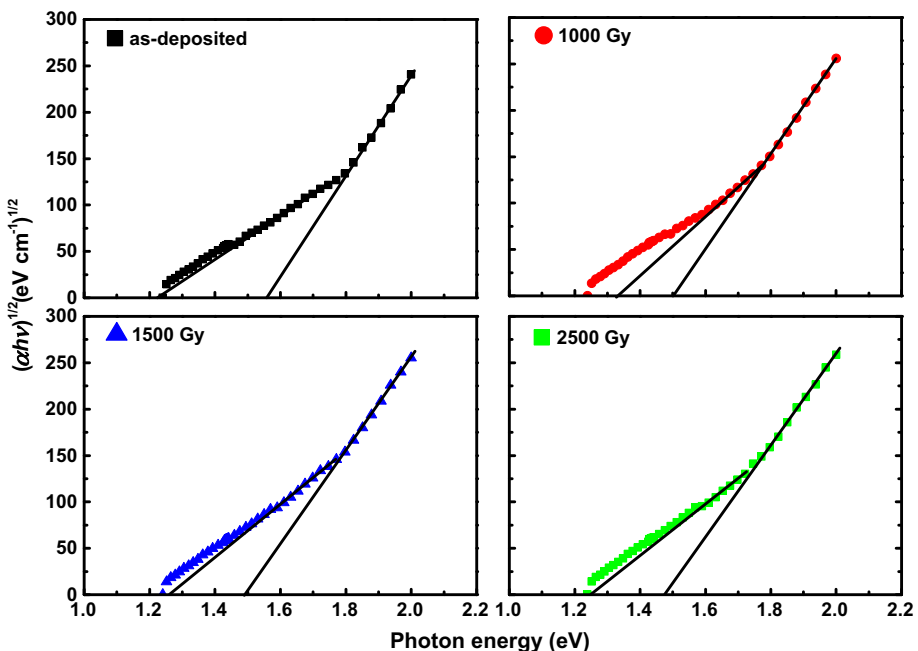


Fig. 8 Variation of $(\alpha h\nu)^{1/2}$ with $(h\nu)$ for as-deposited and irradiated TCVA thin films

Table 2 Absorption parameters of TCVA films

	E_g (eV)	E_{ph} (eV)	E_u (eV)
as-deposited	1.45 ± 0.02	0.114 ± 0.03	0.217 ± 0.02
1000 Gy	1.41 ± 0.01	0.085 ± 0.02	0.237 ± 0.03
1500 Gy	1.38 ± 0.01	0.115 ± 0.03	0.250 ± 0.03
2500 Gy	1.35 ± 0.02	0.110 ± 0.02	0.267 ± 0.02

The absorption edge tail shows the appearance of the localized state, which arises from the indirect transitions within nano-crystalline materials. Urbach et al. (1953) estimated the amount of trailing to a first approximation by plotting the absorption edge data that has been applied to different glassy materials. Figure 9 shows the relation between $\ln(\alpha)$ and the photon energy. The slope inverse yields the value of the tail width, that appears in Table 2. So, we may conclude that the tail width of localized states increases with the increase in the irradiation dose.

The relation between the molar extinction coefficient (ϵ_{molar}) and α is (Schechtman and Spicer 1970):

$$\epsilon_{molar}(\text{L mol}^{-1} \text{cm}^{-1}) = \frac{M\alpha}{\rho \times 10^3 \ln(10)}, \tag{6}$$

where ρ and M are the density of the solid mass and the molecular weight, respectively. The molar extinction coefficient as a photon energy function of TCVA films pre and post irradiation is given in Fig. 10. This figure shows the intensity of the absorption bands due to irradiation. This is attributed to the orientation changing of some electric dipoles through 180° which, consequently results in changing the oscillator strength (Kasha et al. 1965). The ϵ_{molar} has been used to calculate the strength of oscillator (f) and the electric dipole strength (q^2) according to (Kumar et al. 2000):

$$f = 4.32 \times 10^{-2} \int \epsilon_{molar}(v)dv \tag{7}$$

Fig. 9 Dependence of $\ln(\alpha)$ on $h\nu$ for as-deposited and irradiated TCVA films

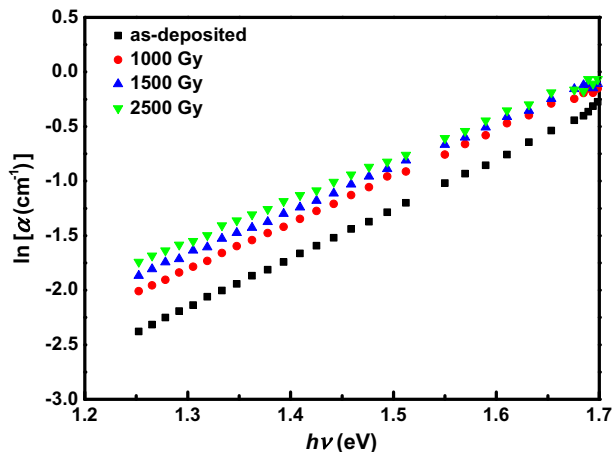


Fig. 10 The molar extinction coefficient (ϵ_{molar}) as a function of photon energy ($h\nu$) for as-deposited and irradiated TCVA films

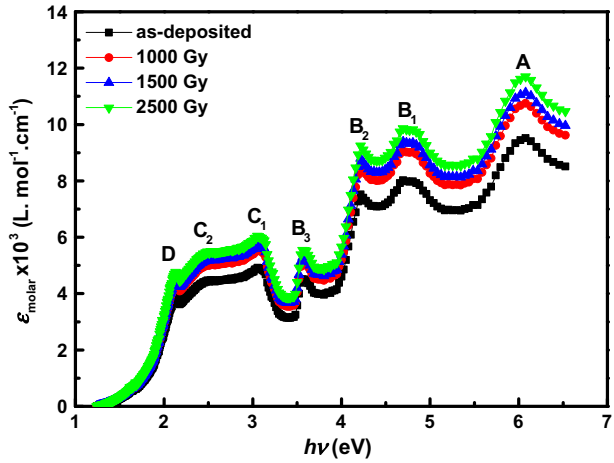


Table 3 The spectral parameters of TCVA film at different bands

Band	q^2 (\AA^2)				f			
	as-dep.	1000 Gy	1500 Gy	2500 Gy	as-dep.	1000 Gy	1500 Gy	2500 Gy
A	0.67	0.70	0.71	0.73	0.30	0.31	0.32	0.33
B ₁	0.20	0.21	0.22	0.23	0.01	0.03	0.04	0.05
B ₂	0.21	0.22	0.24	0.26	0.05	0.06	0.08	0.09
B ₃	0.08	0.09	0.11	0.12	0.01	0.03	0.05	0.07
C ₁	0.60	0.61	0.62	0.64	0.04	0.05	0.06	0.09
C ₂	0.76	0.78	0.80	0.82	0.14	0.16	0.18	0.21
D	0.25	0.26	0.27	0.28	0.05	0.06	0.08	0.09

$$q^2 = \frac{\Delta\lambda}{2500\lambda} \epsilon_{molar} \tag{8}$$

where $\Delta\lambda$ is the absorption half bandwidth and ν is the wavenumber in cm^{-1} . The calculated electric dipole strength and oscillator strength for TCVA pre and post irradiation are listed in Table 3. It can be noted from the table that the absorption transitions in the D-band region have small oscillator strengths due to the opposite directions of the electric dipoles, and the cancellation of electric dipoles that occurs leading to low intensity in the D-bands (Zeyada et al. 2015).

4 Conclusion

The nano-size structure of TCVA films was prepared using the thermal evaporating method. The TCVA thin films show a radiation resistance when exposed to X-ray irradiation up to 2500 Gy. XRD showed that the TCVA films undergoes a transformation from nano-crystalline to amorphous after irradiation. For a dose by 2500 kGy, the optical gap of

TCVA thin film expanded and which could be interpreted as a result of the growth of crystalline disorder and structural bonding deformities. The irradiation acts as to increase the refractive index of the TCVA thin film samples, which may be ascribed to the adjustment in the material's density.

References

- Anthony, J.E., Facchetti, A., Heeney, M., Marder, S.R., Zhan, X.: n-Type organic semiconductors in organic electronics. *Adv. Mater.* **22**, 3876–3892 (2010)
- Arshak, K., Korostynska, O.: Preliminary studies of properties of oxide thin/thick films for gamma radiation dosimetry. *Mater. Sci. Eng. B* **107**, 224–232 (2004)
- Deshpande, A.V., Beidoun, A., Penzkofer, A., Wagenblast, G.: Absorption and emission spectroscopic investigation of cyanovinyl-diethylaniline dye vapors. *Chem. Phys.* **142**, 123–131 (1990)
- Egerton, R., Li, P., Malac, M.: Radiation damage in the TEM and SEM. *Micron* **35**(6), 399–409 (2014)
- El-Mallawany, R., El Rahamani, A.A., Abousehly, A., Yousef, E.: Radiation effect on the ultrasonic attenuation and internal friction of tellurite glasses. *Mater. Chem. Phys.* **52**, 161–165 (1998)
- El-Nahass, M.M., Hassanien, A.M.: Gamma radiation-induced changes on the optical properties of dibenzothio-phenyl-perylene-N, N-dicyclohexylimide thin films. *Radiat. Phys. Chem.* **97**, 178–183 (2004)
- El-Nahass, M.M., Soliman, H.S., Kadry, N., Morsy, A.Y., Yaghmour, S.J.: A new computational method for determining the optical constants and its application for CuInS₂ thin films. *J. Mater. Sci. Lett.* **7**, 1050–1053 (1988)
- El-Nahass, M.M., Soliman, H.S., El-kadry, N., Morsy, A.Y., Yaghmour, S.: A new computational method for determining the optical constants and its application for CuInS₂ thin films. *J. Mater. Sci. Lett.* **7**, 1050–1053 (1997)
- El-Nahass, M.M., Abd-El-Rahman, K.F., Farag, A.A.M., Darwish, A.A.A.: Optical characterisation of thermally evaporated nickel phthalocyanine thin films. *Int. J. Mod. Phys. B* **18**, 421–434 (2004)
- El-Nahass, M.M., Abd-El-Rahman, K.F., Darwish, A.A.A.: Optical properties of organic thin films of 4-tricyanovinyl-N, N-diethylaniline. *Eur. Phys. J. Appl. Phys.* **48**, 200–204 (2009a)
- El-Nahass, M.M., Zeyada, H.M., Abd-El-Rahman, K.F., Darwish, A.A.A.: Fabrication and characterization of 4-tricyanovinyl-N, N-diethylaniline/p-silicon hybrid organic-inorganic solar cells. *Sol. Energy Mater. Sol. Cells* **91**, 1120–1126 (2009b)
- El-Nahass, M.M., Zeyada, H.M., Abd-El-Rahman, K.F., Farag, A.A.M., Darwish, A.A.A.: Fourier-transform infrared and optical absorption spectra of 4-tricyanovinyl-N,N-diethylaniline thin films. *Spectrochimica Acta Part A: Mol Biomol Spectrosc* **69**, 205–210 (2009c)
- El-Nahass, M.M., Darwish, A.A.A., El-Zaidia, E.F.M., Bekheet, A.E.: Gamma irradiation effect on the structural and optical properties of nanostructured InSe thin films. *J. Non-Cryst. Solids* **382**, 74–78 (2013a)
- El-Nahass, M.M., Zeyada, H.M., Abd-El-Rahman, K.F., Darwish, A.: A: Structural characterization and electrical properties of nanostructured 4-tricyanovinyl-N, N-diethylaniline thin films. *Europ. Phys. J. Appl. Phys.* **62**, 10202–10215 (2013b)
- El-Sayed, S.: Electron beam and gamma irradiation effects on amorphous chalcogenide SbSe_{2.5} films. *Nucl. Instrum. Methods Phys. Res. Sect. B* **225**, 535–543 (2004)
- Goetz, K.P., Li, Z., Ward, J.W., Bougher, C., Rivnay, J., Smith, J., Conrad, B.R., Parkin, S.R., Anthopoulos, T.D., Salleo, A., Anthony, J.E.: Effect of acene length on electronic properties in 5-, 6-, and 7-ringed heteroacenes. *Adv. Mater.* **23**, 3698–3703 (2011)
- Hamdalla, T.A., Nafee, S.S.: Radiation effects on the gain of thulium doped fiber amplifier: experiment and modeling. *Opt. Laser Technol.* **55**, 46–49 (2014)
- Haraguchi, K., Li, H.J., Matsuda, K., Takehisa, T., Elliott, E.: Mechanism of forming organic/inorganic network structures during in situ free-radical polymerization in PNIPA—clay nanocomposite hydrogels. *Macromolecules* **38**(8), 3482–3490 (2015)
- Jouhara, H., Vladimir, A., Ibrahim, K.: Potential of heat pipe technology in nuclear seawater desalination. *Desalination* **249**(3), 1055–1061 (2009)
- Kasha, M., Rawls, H.H., Elbauomyi, A.: The exciton model in molecular spectroscopy. *Pure Appl. Chem.* **11**(34), 371–392 (1965)
- Kumar, G., Thomas, J., George, N., Kumar, B., Shnan, P., Poori, V.: Optical absorption studies of free (H₂Pc) and rare earth (RePc) phthalocyanine doped borate glasses. *Phys. Chem. Glass. Eur. J. Glass. Sci. Tech. B* **41**, 89–93 (2000)

- Lehnherr, D., Waterloo, A.R., Goetz, K.P., Payne, M.M., Hampel, F., Anthony, J.E., Jurchescu, O.D., Tykwinski, R.R.: Pure syn-anthradithiophenes: synthesis, properties, and FET performance. *Org. Lett.* **14**, 3660–3663 (2012)
- Mei, Y., Loth, M.A., Payne, M., Zhang, W., Smith, J., Day, C.S.: High mobility field-effect transistors with versatile processing from a small-molecule organic semiconductor. *Adv. Mater.* **25**, 4352–4357 (2013)
- Nafee, S.S., Hamdalla, T.A., Shaheen, S.A.: FTIR and optical properties for irradiated PVA–GdCl₃ and its possible use in dosimetry. *Phase Transit.* **90**(5), 439–448 (2017)
- Schechtman, B., Spicer, W.: Near infrared to vacuum ultraviolet absorption spectra and the optical constants of phthalocyanine and porphyrin films. *J. Mol. Spectrosc.* **33**, 28–48 (1970)
- Urbach, F.: The Long-wavelength edge of photographic sensitivity and of the electronic absorption of solids. *Phys. Rev.* **92**, 1324–1330 (1953)
- Zeyada, H.M., Makhoulf, M.M., El-Nahass, M.M.: Influence of gamma ray irradiation and annealing temperature on the optical constants and spectral dispersion parameters of metal-free and zinc tetraphenylporphyrin thin films: a comparative study. *Spectrochimica Acta Part A* **148**, 338–347 (2015)